 CMC, vol.23, no.2, pp.135-153, 2011

# Application of the Method of Fundamental Solutions and the Generalized Lagally Theorem to the Interaction of Solid Body and External Singularities in An Inviscid Fluid

**C. T. Wu[1], F.-L. Yang[2] and D. L. Young[3]**

**Abstract:** This paper proposes a method that can calculate the hydrodynamic force of a non-circular object in an inviscid, irrotational, and incompressible flow with the presence of external flow singularities. In order to handle irregular object, the method of fundamental solutions (MFS) is employed to numerically construct the singularity system that describes the body and the flow motion and meets the boundary condition. The obtained singularity system is then integrated into the generalized Lagally theorem to compute the instantaneous hydrodynamic force via algebraic calculations and to describe the unsteady interaction of the object and its ambient flow. The proposed method is validated by simulating the interaction of a circular cylinder with an external free vortex and the numerical solutions are compared to the literature theoretical descriptions. The time history of the cylinder and the vortex trajectory can be exactly reproduced. The current method is then employed to study the axisymmetric approach of a vortex pair–two free vortices with opposite strengths–towards a neutrally buoyant ellipse. We show how the vortex pair and the ellipse trajectory changes with respect to different vortex configurations and ellipse aspect ratios. This example demonstrates the capability of the current method in dealing with fluid-body interaction problem, especially for irregular body shape.

**Keywords:** potential flows, fluid-body interaction, Lagally theorem, method of fundamental solutions.

## 1 Introduction

The hydrodynamic force on a solid object that moves in an unbounded incompressible flow and its interaction with the ambient flow have been a research topic of

[1] Department of Civil Engineering, National Taiwan University, Taipei, Taiwan.
[2] Department of Mechanical Engineering, National Taiwan University, Taipei, Taiwan.
[3] Department of Civil Engineering, National Taiwan University, Taipei, Taiwan. Corresponding author, dlyoung@ntu.edu.tw.

fundamental fluid mechanics. When vorticity is confined in flow regimes that are much smaller than the size of the immersed body or the flow domain, the fluid motion can be approximated as an ideal flow governed by the Laplace equation. The confined vorticity may be approximated as a vortex singularity of matching circulation, being its strength multiplied $2\pi$. By superposing specific fundamental solutions of the Laplace equation, the desired flow potential function can be generated which meets the boundary condition of no-penetration. The hydrodynamic force on the body can then be obtained by integrating the pressure around the body as described by the Bernoulli equation [Lamb (1932); Milne-Thompson (1968); Yih (1977)].

Lagally (1922) proposed a theorem that gives the steady hydrodynamic force and torque on a three-dimensional fixed rigid body in an inviscid and incompressible flow with external sources or dipoles. The force and torque can be obtained by straightforward algebraic manipulations of the strengths and the positions of the external singularities which bypasses the surface integral of the potential function in conventional Blasius theorem. The work was later extended by Cummins (1953) to consider unsteady flow motion. Later on, Landweber and Yih (1956) took an alternative but powerful approach to derive the formulae by considering the singularities *within* a three-dimensional body and their results can be applied to the problem with multiple solid bodies. The theorem for the case with deformable bodies and multipoles in unsteady flow was considered by Landweber and Miloh (1980), and a shorter and simpler derivation for translational motion was given by Biesheuvel (1985). Based on the framework of Landweber and Yih (1956), the generalized Lagally theorem that considers the presence of vortex singularity in two-dimensions was derived by Wu, Yang, and Young (2011) in terms of complex variable. These authors also connected their results to the Taylor theorem [Taylor (1928); Birkhoff (1950); Landweber (1956); Landweber and Yih (1956); Landweber and Chwang (1989)] that expresses the added mass coefficients for a body moving in an unbounded ideal flow in terms of the strengths and configurations of its internal singularities adopted to describe the flow field induced by the body motion.

However, the precise strengths and positions of the internal image singularities are in general unknown for a body of irregular shape. This difficulty can be resolved numerically by implementing the method of fundamental solutions (MFS). The MFS is a boundary type meshless numerical method developed for problems governed by some linear operator. The fundamental solutions (or Green's functions) of the operator are utilized at some singular points outside of the problem domain in a manner that approximates the solution with their superposition. The boundary condition is then enforced at finite numbers of collocation points on the boundary to determine the weightings or the locations of the selected fundamental solutions [Fairweather and Karageorghis (1998); Golberg and Chen (1998); Fairweather, Karageorghis, and Martin (2003); Young, Tsai, Lin, and Chen (2006); Gu, Young, and Fan (2009); Lin, Gu, and Young (2010)]. For two-dimensional Lapalce operator and Neumann type boundary condition, the fundamental solution is that represents a unit source in the potential flow theory. They are superposed with weightings determined to ensure a no-penetration boundary condition which generates a singularity system whose strength and configuration can be utilized to estimate the hydrodynamic force on the solid object by the generalized Lagally theorem. This concept has be implemented numerically in this work, targeting flow-body interaction with an object of irregular shape.

In the following section 2, the two-dimensional Lagally theorem is briefly introduced following Wu, Yang, and Young (2011). In section 3, the general formulation with the MFS is given and two numerical examples such as the interaction of a circular cylinder with a free vortex and the axisymmetric approach of a vortex pair with an elliptical cylinder of different aspect ratios are studied in section 4. Section 5 summarizes this work and comments on possible directions for future research.

## 2 The generalized Lagally theorem

Consider a two-dimensional solid object that translates at velocity $\mathbf{U}$ and rotates with angular velocity $\Omega$ relative to an inertial frame $OX_1X_2$ fixed in an unbounded inviscid and incompressible fluid at rest at infinity as depicted in Fig. 1. The position vector of a point $Q$ with respect to $O$ and the translational velocity of the object take the form $\mathbf{X} = X_1\mathbf{e}_1 + X_2\mathbf{e}_2$ and $\mathbf{U} = U_1\mathbf{e}_1 + U_2\mathbf{e}_2$ where $(\mathbf{e}_1, \mathbf{e}_2)$ are the unit vectors alone $OX_1$ and $OX_2$ axes. The resulting flow is irrotational with respect to $OX_1X_2$ and can be described by the negative spatial gradient of a velocity potential function, $\phi$, which satisfies the Laplace equation

$$\nabla^2\phi = 0. \tag{1}$$

The no-penetration boundary condition on the body surface can be expressed as

$$-\frac{\partial\phi}{\partial n} = \mathbf{v}\cdot\mathbf{n} = [\mathbf{U} + \Omega\times(\mathbf{X} - \mathbf{X}_o)]\cdot\mathbf{n}, \tag{2}$$

where $\mathbf{v} = v_1\mathbf{e}_1 + v_2\mathbf{e}_2$ is the fluid velocity, $\mathbf{n} = n_1\mathbf{e}_1 + n_2\mathbf{e}_2$ is the unit normal vector pointing from the object surface into the fluid, and $\mathbf{X}_o = X_{o1}\mathbf{e}_1 + X_{o2}\mathbf{e}_2$ is the position vector of a point $o$ fixed on the object.

In terms of complex variable $z = X_1 + iX_2$, a complex velocity potential, $w = \phi + i\psi$, can be formulated with $\psi$ denoting the stream function. Now, the velocity field is

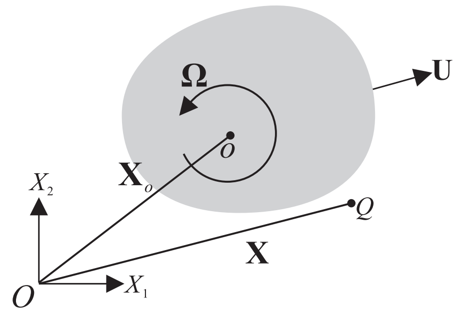


Figure 1: Schematic sketch of the inertial frames of reference, $OX_1X_2$. $Q$ is point of interest with position vector $\mathbf{X} = X_1\mathbf{e}_1 + X_2\mathbf{e}_2$ and $\mathbf{X}_o = X_{o1}\mathbf{e}_1 + X_{o2}\mathbf{e}_2$ is the position vector of a point $o$ fixed on the object with respect to the inertial frame.

obtained by $\bar{v} = -dw/dz = v_1 - iv_2$ where the bar over a complex variable denotes its conjugate. The complex velocity potential can be decomposed into

$$w = \sum_{\alpha=1}^{3} U_\alpha w_\alpha + w_{\text{ext}} + w_{\text{int}}, \tag{3}$$

where the first group represents the body translation, $(U_1, U_2)$, and rotation, $U_3 = \Omega$, with corresponding *normalized* potentials, $w_\alpha$. The second group are functions employed exterior to the body to represent specific ambient flow structure or motions of other coexisting bodies. The last group are internal potential functions adopted with respect to the external singularities to ensure the no-penetration boundary condition [Landweber and Yih (1956)]. With this potential decomposition, the no-penetration boundary condition, Eq. (2), may be separated into

$$\text{Re}\left[-\frac{dw_\alpha}{dz}(n_1 + in_2)\right] = n_\alpha, \text{ for } \alpha = 1,2,3, \tag{4a}$$

and

$$\text{Re}\left[(-\frac{dw_{\text{ext}}}{dz} - \frac{dw_{\text{int}}}{dz})(n_1 + in_2)\right] = 0, \tag{4b}$$

where the preceding Re denotes the real part of a complex function and $n_3 = (X_1 - X_{o1})n_2 - (X_2 - X_{o2})n_1$.

The hydrodynamic force on the body can be calculated by integrating the hydrodynamic pressure, $p$, around the body as $F = F_1 + iF_2 = i\int_{\mathscr{C}} p\,dz$ with $\mathscr{C}$ denoting the object surface. Substituting the unsteady Bernoulli equation for $p$, the force on a moving body can be obtained, with respective to the fixed inertial frame $OX_1X_2$, as

$$F = -\frac{1}{2} i\rho \overline{\int_{\mathscr{C}} \left(\frac{dw}{dz}\right)^2 dz} - \frac{d}{dt}\sum_{\alpha=1}^{3}\left[U_\alpha \left(A_{\alpha 1} + iA_{\alpha 2}\right)\right] + i\rho \frac{d}{dt}\int_{\mathscr{C}} w_{\text{int}}\, dz, \tag{5}$$

where $\rho$ is the fluid density. The first term on the right hand side of Eq. (5) is dynamically equivalent to the quasi-steady force derived from the conventional Blasius theorem [Milne-Thompson (1968)]. The second term is the added mass force resulting from the rate of change of fluid impulse due to unsteady object motion and $(A_{\alpha 1}, A_{\alpha 2})$ are the added mass coefficients. In general, the added mass coefficients are not constant since the object orientation may change if it rotates. Note that the Taylor theorem can be applied to compute the added mass coefficients with algebraic manipulations of the strengths and the positions of the unit potential functions, $w_\alpha$, in Eq. (3) [Taylor (1928); Birkhoff (1950); Landweber (1956); Landweber and Yih (1956); Landweber and Chwang (1989)]. The last term results from the temporal variation of the strengths and configurations of the internal image singularities generated when the object exhibits relative motion to its ambient external singularities.

Let there be sources, vortices, and dipoles exterior to the object in the flow field, which requires different sets of internal image singularities to ensure the boundary condition of no-penetrating flow. The contour integrals of the first and the last term on the right hand side of Eq. (5) can be integrated by the residue theorem to yield the final force formula as

$$\begin{aligned} F = &-2\pi\rho \sum_{j,\text{all}} \overline{\left(\mu_j \left.\frac{df}{dz}\right|_{Z_j^{(d)}} + m_j f|_{Z_j^{(s)}} - i\kappa_j f|_{Z_j^{(v)}}\right)} \\ &- \frac{d}{dt}\sum_{\alpha=1}^{3}\left[U_\alpha \left(A_{\alpha 1} + iA_{\alpha 2}\right)\right] - 2\pi\rho \frac{d}{dt}\sum_{j,\text{int}} \left(\mu_j + m_j Z_j^{(s)} - i\kappa_j Z_j^{(v)}\right), \end{aligned} \tag{6}$$

where $\left(\mu_j, Z_j^{(d)}\right)$, $\left(m_j, Z_j^{(s)}\right)$, and $\left(\kappa_j, Z_j^{(v)}\right)$ are the strength and position of dipole, source and vortex within the body, respectively. The function $f = -dw_{\text{ext}}/dz|_{Z_j}$ in the first summation is the flow velocity induced by all the singularities exterior to the object considered at an internal singularity $Z_j$ and will be referred to as the *partial velocity function*. Note that the first summation in Eq. (6) is executed on *all* the singularities *within* the body. However, the last group contains *only* the contributions of the internal *image* singularities, $w_{\text{int}}$, and any temporal variation of these singularity strengths or positions can result in an unsteady force. The ones employed to generate the body motion are excluded since their effects have been accounted for by the added mass force.

In this section, we have briefly introduced the generalized Lagally theorem, Eq. (6), and more detailed derivations can be found in Wu, Yang, and Young (2011). Next, we describe how the MFS can be implemented to solve for the strengths and the positions of the internal singularities for an object of non-circular shape.

## 3 Formulation with the MFS

### *3.1 The method of fundamental solutions for exterior domain problems*

Let $\mathscr{D}_0 \subset \mathbb{R}^2$ be a bounded domain with boundary $\Gamma$ and $\mathscr{D} = \mathbb{R}^2 - (\mathscr{D}_0 \cup \Gamma)$ is the domain of interest (the unshaded area in Fig. 2). Consider a boundary value problem

$$L(\phi) = 0, \text{ in } \mathscr{D}, \tag{7a}$$

and

$$B(\phi) = B_0, \text{ on } \Gamma, \tag{7b}$$

where $L$ and $B$ are linear operators and $B_0$ is a given function. Let $P = (X_1, X_2)$ be a point in $\mathscr{D}$ and $K(P, Q_j)$ be the fundamental solution of the linear operator $L$ with a singularity $Q_j$ lie in $\mathscr{D}_0$, which satisfies

$$L[K(P, Q_j)] = -\delta(P - Q_j), \tag{8}$$

where $\delta$ is the Dirac delta function. In the MFS, a numerical solution of $\phi$ at $P$ can be approximated by superposing $N$ fundamental solutions $K(P, Q_j)$ with respective singularities at $Q_j$ as

$$\phi_N(\mathbf{c}, \mathbf{Q}; P) = \sum_{j=1}^{N} c_j K(P, Q_j), \tag{9}$$

where $\mathbf{c} = [c_1, c_2, \ldots, c_N]^T$ are the weighting coefficients of the fundamental solutions and $\mathbf{Q}$ is a $2N$-vector formed by the sequence of $Q_j = (X_{j1}, X_{j2})$.

In conventional MFS, $N$ singularities $Q_j$ are first assigned within $\mathscr{D}_0$ in an user-specified manner. The required boundary condition on the object surface, $\Gamma$, is then employed to determine the unknown coefficients, $\mathbf{c}$, with the *boundary collocation method*. In this method, $M$ collocation points $\tilde{P}_k$ are first distributed evenly on $\Gamma$ where the boundary condition, Eq. (7b), is enforced on each collocation point by Eq. (9) to give

$$\sum_{j=1}^{N} c_j B\left[K(\tilde{P}_k, Q_j)\right] = B_0(\tilde{P}_k), \text{ for } k = 1, \ldots, M, \tag{10}$$

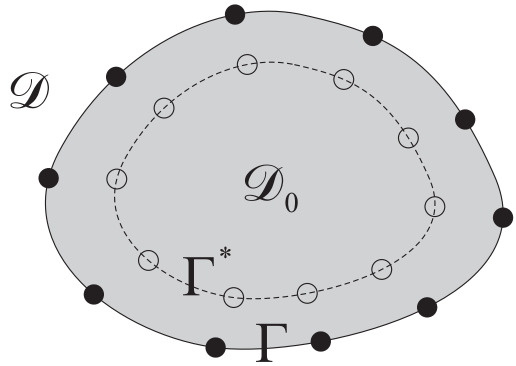


Figure 2: Decomposition of the problem domains, $\mathscr{D}$ and $\mathscr{D}_0$. The object and the pseudo inner boundaries are $\Gamma$ and $\Gamma^*$ on which the collocation points (solid circles) and inner sources (open circles) are evenly distributed.

which forms a linear system

$$\mathbf{B}\mathbf{c} = \mathbf{B}_0, \tag{11}$$

where $\mathbf{B}$ is a $M$-by-$N$ matrix with entry $B_{kj} = B[K(\tilde{P}_k, Q_j)]$ and $\mathbf{B}_0 = [B_0(\tilde{P}_1), \ldots, B_0(\tilde{P}_M)]^T$. When $M = N$, the linear system can be solved by the Gaussian elimination; when $M > N$, a linear least squares system can be formulated and solved by conventional routines. Once the coefficients are solved, the approximated solution for any point in $\mathscr{D}$ can be calculated by Eq. (9) [Fairweather and Karageorghis (1998); Golberg and Chen (1998); Fairweather, Karageorghis, and Martin (2003); Young, Tsai, Lin, and Chen (2006); Gu, Young, and Fan (2009); Lin, Gu, and Young (2010)]. However, the distribution of the source points is one of the main difficulties of the MFS which plays a crucial role regarding the accuracy of the solution.

Thus, $\mathbf{Q}$ is not pre-assigned in this work but treated as unknown like $\mathbf{c}$ [Johnston and Fairweather (1984); Wang, Ahmed, and Leavers (1990)]. The boundary equations are translated into $M$ nonlinear equations with $3N$ unknowns, $\{c_j, X_{j1}, X_{j2} | j = 1, \ldots, N\}$, and thus cannot be solved as a conventional linear system. We adopt a nonlinear least squares optimization technique to determine $\mathbf{c}$ and $\mathbf{Q}$ simultaneously by minimizing the total deviation between the approximated and the exact boundary conditions at $M$ collocation points. This quantity is calculated by

$$\tau_{tol}(\mathbf{c}, \mathbf{Q}) = \sum_{k=1}^{M} \left[ \sum_{j=1}^{N} c_j B\left(K(\tilde{P}_k, Q_j)\right) - B_0(\tilde{P}_k) \right]^2, \tag{12}$$

and a desired tolerance is chosen to be $\tau_{tol} = 1E-6$. This work adopts UNLSJ, a Fortran IMSL Library subroutine, which iteratively solves a nonlinear least squares problem using an initial assignment of $\mathbf{c}_0$ and $\mathbf{Q}_0$ by the modified Levenberg-Marquardt algorithm and an user-supplied Jacobian [Moré, Garbow, and Hillstrom (1980)].

In this application, we chose $\mathbf{c}_0 = 0$ and $\mathbf{Q}_0$ are evenly distributed along a pseudo boundary, $\Gamma^*$, chosen to be similar to $\Gamma$ but half of its size as depicted in Fig. 2. The collocation points are distributed similar to $\mathbf{Q}_0$ on the object boundary $\Gamma$. Since we are dealing with a nonlinear least squares problem with $3N$ unknowns, the number of the collocation points $M = 9N$ is used. Further, since the configurations as well as the strengths of the interior singularities are sought by Eq. (12) at each time step, the solutions at $n$ step are used as the initial guesses for $n+1$ step to enhance the iteration efficiency.

### 3.2 Solutions of the potential flow problems by the MFS

The two-dimensional motion of an inviscid and incompressible flow is governed by the Laplace equation whose fundamental solution, with singularity at $Q_j$, is

$$K(P,Q_j) = -\frac{1}{2\pi}\ln|P-Q_j|, \tag{13}$$

where $|P-Q_j|$ is the distance between points $P$ and $Q_j$. To conform with the notation in the generalized Lagally theorem, Eq. (13) can be transformed into complex variable by replacing $|P-Q_j|$ with $(z-Z_j)$. The weighting coefficient $c_j$ in Eq. (9) clearly represents the strength of a point source in the classical potential flow theory. However, this is not a feasible basis function for an external flow problem since the logarithmic function diverges at infinity. Thus, a modified fundamental solution is adopted, following Katsurada (1989), as

$$\tilde{K}(P,Q_j) = -\frac{1}{2\pi}\ln\frac{(z-Z_j)}{(z-Z_c)}, \tag{14}$$

where $Z_c$ is the geometric center of $\mathscr{D}_0$. Eq. (14) is equivalent to having two sources with opposite strengths at $Z_j$ and $Z_c$ and the mass conservation is thus automatically satisfied. It can be shown that this modified fundamental solution converges as $O(1/|z|)$ when $|z| \to \infty$.

Now, let a non-rotating solid object move at velocity $U = U_1 + iU_2$ with the presence of $\tilde{N}_v$ free vortices of strengths $\tilde{\kappa}_k$ at $\tilde{Z}_k^{(v)}$. Note that only the formulation with the free vortex is presented and those for the other singularities can be derived similarly. Further, for clear derivation, all the variables not belonging to $\mathscr{D}_0$ (the body interior) will be denoted with overhead tilde. The velocity potential for the resulting flow can be developed by using Eqs. (3), (9), and (14), as

$$w_N(z) = \left[-U_1 \sum_{j=1}^{N_1} m_j^{(1)} \ln \frac{(z - Z_j^{(1)})}{(z - Z_c)} - U_2 \sum_{j=1}^{N_2} m_j^{(2)} \ln \frac{(z - Z_j^{(2)})}{(z - Z_c)}\right] + i \sum_{j=1}^{\tilde{N}_v} \tilde{\kappa}_j \ln(z - \tilde{Z}_j^{(v)}) + i \sum_{j=1}^{N_v} \kappa_j \ln \frac{(z - Z_j^{(v)})}{(z - Z_c)}. \quad (15)$$

Here, $N_1$ and $N_2$ sources are employed separately to represent the object motion along $\mathbf{e}_1$ and $\mathbf{e}_2$, respectively, and the corresponding strengths and locations are denoted by $m_j^{(1),(2)}$ and $Z_j^{(1),(2)}$ using distinctive superscripts. $N_v$ is the number of the internal vortices used to counterbalance the flux generated by the $\tilde{N}_v$ exterior free vortices. Now, the decomposed no-penetration boundary conditions, Eqs. (4a) and (4b), are imposed on the $M$ boundary collocation points, $\tilde{Z}_k$, using Eq. (15) to give

$$\sum_{j=1}^{N_1} m_j^{(1)} \left[\frac{(\tilde{X}_{k1} - X_{j1}^{(1)})n_1 + (\tilde{X}_{k2} - X_{j2}^{(1)})n_2}{|\tilde{Z}_k - Z_j^{(1)}|^2} - \frac{(\tilde{X}_{k1} - X_{c1})n_1 + (\tilde{X}_{k2} - X_{c2})n_2}{|\tilde{Z}_k - Z_c|^2}\right] = n_1, \quad (16a)$$

$$\sum_{j=1}^{N_2} m_j^{(2)} \left[\frac{(\tilde{X}_{k1} - X_{j1}^{(2)})n_1 + (\tilde{X}_{k2} - X_{j2}^{(2)})n_2}{|\tilde{Z}_k - Z_j^{(2)}|^2} - \frac{(\tilde{X}_{k1} - X_{c1})n_1 + (\tilde{X}_{k2} - X_{c2})n_2}{|\tilde{Z}_k - Z_c|^2}\right] = n_2, \quad (16b)$$

and

$$\sum_{j=1}^{N_v} \kappa_j \left[\frac{(\tilde{X}_{k1} - X_{j1}^{(v)})n_2 - (\tilde{X}_{k2} - X_{j2}^{(v)})n_1}{|\tilde{Z}_k - Z_j^{(v)}|^2} - \frac{(\tilde{X}_{k1} - X_{c1})n_2 - (\tilde{X}_{k2} - X_{c2})n_1}{|\tilde{Z}_k - Z_c|^2}\right] = - \sum_{j=1}^{\tilde{N}_v} \tilde{\kappa}_j \frac{(\tilde{X}_{k1} - \tilde{X}_{j1}^{(v)})n_2 - (\tilde{X}_{k2} - \tilde{X}_{j2}^{(v)})n_1}{|\tilde{Z}_k - \tilde{Z}_j^{(v)}|^2}, \quad (16c)$$

for $k = 1, \ldots, M$.

With initial guesses, $m_{j0}^{(1)}$ and $Z_{j0}^{(1)}$, the iteration schemes commence to find a solutions of Eq. (16a) that satisfies the error threshold, $\tau_{tol} = 1E - 6$. Similar iteration procedures were also performed for Eqs. (16b) and (16c) to determine $(m_j^{(2)}, Z_j^{(2)})$ and $(\kappa_j, Z_j^{(v)})$. Note that Eqs. (16a) and (16b) depend only on the object geometry and so do their solutions, $(m_j^{(1)}, Z_j^{(1)})$ and $(m_j^{(2)}, Z_j^{(2)})$, that can be employed to calculate the approximate added mass coefficients [Yang, Wu, and Young (2011)].

Hence these coefficients also change with the body geometry, agreeing to the classical potential theory [Lamb (1932); Milne-Thompson (1968); Yih (1977)]. Note that the effect of a dipole in the potential flow theory is approximated here by multiple sources which can bear opposite strengths. Though the addition of singularities seem to complicate the mathematical description and thus may degrade computation efficiency, it is worth reminding that the current formulation is designed in particular for non-circular object.

Once a set of the internal singularities are solved, the hydrodynamic force on the object can be calculated by the generalized Lagally theorem, Eq. (6), to give the equation of motion for the object as

$$\gamma m_d \frac{d^2 Z_c}{dt^2} = -2\pi\rho \left[ \overline{\sum_{j=1}^{N_1} U_1 m_j^{(1)} \left( f|_{Z_j^{(1)}} - f|_{Z_c} \right)} + \overline{\sum_{j=1}^{N_2} U_2 m_j^{(2)} \left( f|_{Z_j^{(2)}} - f|_{Z_c} \right)} \right. \\ \left. + i \overline{\sum_{j=1}^{N_v} \kappa_j \left( f|_{Z_j^{(v)}} - f|_{Z_c} \right)} \right] - \frac{d}{dt} \sum_{\alpha=1}^{2} \left[ U_\alpha (A_{\alpha 1} + i A_{\alpha 2}) \right] + i 2\pi\rho \frac{d}{dt} \sum_{j=1}^{N_v} \kappa_j \left( Z_j^{(v)} - Z_c \right), \tag{17}$$

where $\gamma = \rho_s/\rho$ is the density ratio between solid and liquid, $m_d$ is the displaced fluid mass, and the partial velocity function is $f(z) = -i \sum_{j=1}^{\tilde{N}_v} \tilde{\kappa}_j / (z - \tilde{Z}_j^{(v)})$. The external vortex moves at the flow velocity induced by *all* the other singularities at $z = \tilde{Z}_k^{(v)}$ as

$$\overline{\frac{d\tilde{Z}_k^{(v)}}{dt}} = i \sum_{\substack{j=1 \\ j \neq k}}^{\tilde{N}_v} \tilde{\kappa}_j \left( \frac{1}{\tilde{Z}_k^{(v)} - \tilde{Z}_j^{(v)}} \right) - i \sum_{j=1}^{N_v} \kappa_j \left( \frac{1}{\tilde{Z}_k^{(v)} - Z_j^{(v)}} - \frac{1}{\tilde{Z}_k^{(v)} - Z_c} \right) \\ - U_1 \sum_{j=1}^{N_1} m_j^{(1)} \left( \frac{1}{\tilde{Z}_k^{(v)} - Z_j^{(1)}} - \frac{1}{\tilde{Z}_k^{(v)} - Z_c} \right) + U_2 \sum_{j=1}^{N_2} m_j^{(2)} \left( \frac{1}{\tilde{Z}_k^{(v)} - Z_j^{(2)}} - \frac{1}{\tilde{Z}_k^{(v)} - Z_c} \right), \tag{18}$$

for $k = 1, \ldots, \tilde{N}_v$. Eq. (18) is further employed to simplify the first group on the right hand side of Eq. (17) to obtain $i2\pi\rho \sum_{k=1}^{\tilde{N}_v} \tilde{\kappa}_k d\tilde{Z}_k^{(v)}/dt$. Eq. (17) can be integrated in time once to give

$$\gamma m_d \frac{dZ_c}{dt} + \sum_{\alpha=1}^{2} \left[ U_\alpha (A_{\alpha 1} + i A_{\alpha 2}) \right] - i2\pi\rho \sum_{j=1}^{\tilde{N}_v} \tilde{\kappa}_j \tilde{Z}_j^{(v)} - i2\pi\rho \sum_{j=1}^{N_v} \kappa_j \left( Z_j^{(v)} - Z_c \right) = L_0, \tag{19}$$

where the integral constant, $L_0$, represents the system total momentum that remains constant. In addition to the object momentum in the first term, the following three terms represent the fluid impulses generated by the object motion, the external free vortices and the internal image vortices, respectively. Finally, the $\tilde{N}_v$ equations in Eq. (18), and Eq. (19) are solved by the fourth-order Runge-Kutta method to study the object-vortex interaction. All the cases presented in this work are computed with a constant time increment, $\Delta t = 0.01$.

## 4 Examples

To validate the current formulation, we first consider the interaction between a circular cylinder and a free vortex. Next, we study the axisymmetric approach of a vortex pair towards an elliptical cylinder of different aspect ratios to demonstrate the capability of the proposed method.

### *4.1 Interaction between a circular cylinder and a free vortex*

Consider a stationary solid circular cylinder of radius $a$ and density $\rho_c$ initially at $Z_c = 0$ that is free to move in response to a nearby free vortex of strength $\tilde{\kappa}$ at $\tilde{Z}^{(v)} = D$. The system behavior has been investigated theoretically by Eames, Landeryou, and Flór (2007) where the equations of motion for both the free vortex and the cylinder are given explicitly by integrating the associated potential functions to obtain the desired flow impulses. The same equation of motion for the cylinder can be derived by the current Lagally theorem, Eq. (6), using the following singularities. Firstly, two image vortices with strengths $\kappa$ and $-\kappa$ are located at $Z_c$ and $Z_i$, respectively, with $Z_i = Z_c + a^2/l^2(\tilde{Z}^{(v)} - Z_c)$ being the inverse point of $\tilde{Z}^{(v)}$ with respect to $Z_c$ and $l = |\tilde{Z}^{(v)} - Z_c|$. The non-zero added mass coefficients for circular cylinder are $A_{11} = A_{22} = \rho\pi a^2$ [Lamb (1932); Milne-Thompson (1968); Yih (1977)] that remain the same during the system evolution due to spherical symmetry. With the singularity strengths and positions, Eq. (19) can be manipulated to give

$$(\rho_c + \rho)\pi a^2 \frac{dZ_c}{dt} - i2\pi\rho\tilde{\kappa}\tilde{Z}^{(v)} + i2\pi\rho\tilde{\kappa}\frac{a^2}{\bar{Z}} = L_0, \tag{20}$$

where $Z = \tilde{Z}^{(v)} - Z_c$ [Wu, Yang, and Young (2011)].

In the formulation of the MFS, $N = N_1 = N_2 = N_v = 12$ was used in Eq. (15). Initial guesses are set to $m_{0j}^{(1)} = m_{0j}^{(2)} = \kappa_{0j} = 0$ and $Z_{0j}^{(1)} = Z_{0j}^{(2)} = Z_{0j}^{(v)} = 0.5r(\alpha)e^{i\alpha}$, $r(\alpha) = a$, $\alpha = 2\pi(j-1)/N + \pi/N$, for $j = 1,\ldots,N$ when solving Eqs. (16a), (16b) and (16c). The collocation points are uniformly distributed on the boundary according to $\tilde{Z}_k = r(\beta)e^{i\beta}$, $\beta = 2\pi(k-1)/M + \pi/M$, for $k = 1,\ldots,M = 9N$. Since Eqs. (16a) and (16b) only depend on the body geometry, the strengths and the locations relative to the cylinder center of the internal sources, $m_j^{(1),(2)}$ and $Z_j^{(1),(2)} -$

$Z_c$, remain the same. Thus, iterations were performed on Eqs. (16a) and (16b) to obtain the source distributions only at the beginning of system evolution. The source locations at later times, $Z_j^{(1)}$ and $Z_j^{(2)}$, are updated from the corresponding $Z_c$. However, since the relative position of the free vortex and the cylinder, $\tilde{Z}^{(v)} - Z_c$, varies in time, Eq. (16c) is solved at every time step to update the image vortices locations using the solutions from the previous step as the initial conditions.

Once the strengths and the positions of the singularities at one time step are solved, the equations of motion for both the cylinder and the vortex, Eqs. (19) and (18), are numerically integrated. The resulting trajectories of the vortex and the cylinder center are shown in Figs. 3(i) and (ii), respectively, where two solid-to-fluid density ratio, $\gamma = \rho_c/\rho = 200$ and 1000, are used for cases (a) and (b). Here, zero initial total momentum, $L_0 = 0$, is adopted following Eames, Landeryou, and Flór (2007) and good agreement with their Figs. 1(a) and (c) is obtained. Further, to ensure identical time history, the square of the separation between the cylinder and the vortex, $|Z|^2 = |\tilde{Z}^{(v)} - Z_c|^2$, is examined in time for both $\gamma$ in Fig. 4 and the data obtained from the current MFS (shown by the dots) agree to the theoretical predictions by Eq. (20) (shown by the lines). It is observed that the slight deduction of $\gamma$ results in dramatic increase of oscillation amplitude and slight extension of period.

### *4.2 Axisymmetric approach of a vortex pair towards an elliptical cylinder*

To demonstrate the capability of the current method in handling non-circular object, the normal approach of a vortex pair of opposite strengths towards a neutrally buoyant elliptical cylinder is considered, as depicted in Fig. 5. The cylinder has a semi-major and minor axes of $a$ and $b$ and is located at $Z_c$ in an inertial reference frame. The vortices are at $Z_v$ and $\overline{Z_v}$, each possessing a horizontal and a vertical distance, $h$ and $d$, from $Z_c$. The upper and the lower vortex strength is $\kappa$ and $-\kappa$, respectively.

Kanso and Oskouei (2008) has considered the same system with a focus on the *relative equilibria* between the vortex and the cylinder, which is defined as the relative position when the vortex remains stationary in the reference frame moving with the cylinder. Two families of relative equilibria are found–the moving Föppl equilibria and the equilibria along the axis perpendicular to the direction of motion. The equilibria stability was revealed which differ significantly from the classical Föppl equilibria [Shashikanth (2006)]. Here, we study the dynamic interaction between the two with the cylinder initially at rest and a vortex pair approaching from upstream at a distance $d(0) = 10\sqrt{ab}$. The number of internal singularities is $N = N_1 = N_2 = N_v = 16$ and their initial states are assigned similar to the previous

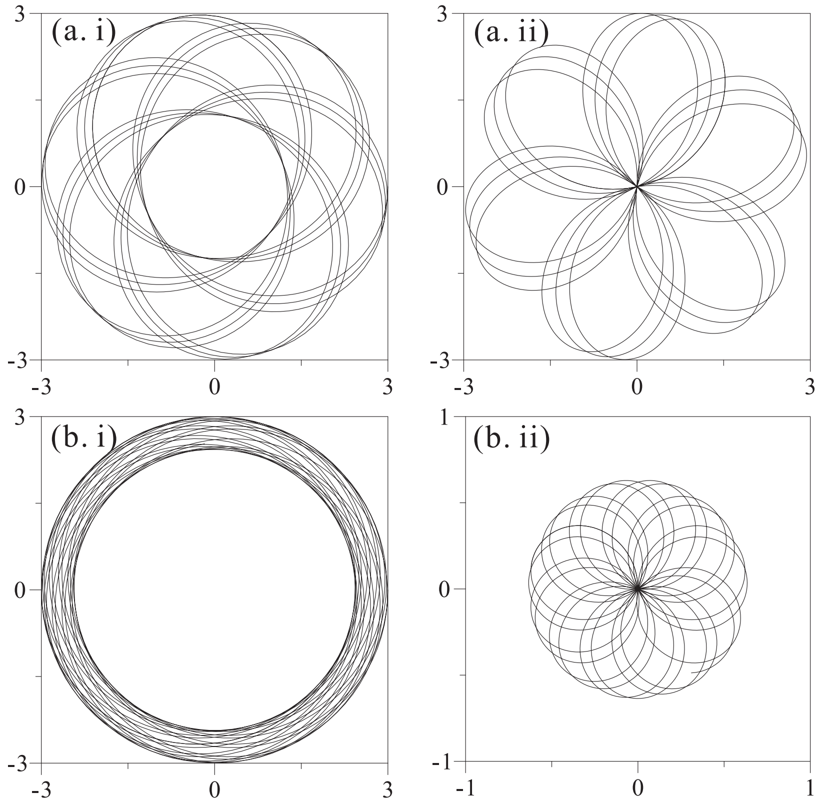


Figure 3: The trajectories of the point vortex (left, i) and the cylinder center (right, ii) for two solid-to-liquid density ratios $\gamma =$ (a)200; (b)1000. The initial separation between vortex and cylinder center is three cylinder radii.

case but using $r(\alpha) = ab/\sqrt{a^2 \sin^2 \alpha + b^2 \cos^2 \alpha}$. Similarly, the $M = 9N$ collocation points are distributed evenly as depicted in Fig. 5.

The resulting strengths and positions of the singularities as well as the non-zero added mass coefficients, $A_{11} = \rho \pi b^2$ and $A_{22} = \rho \pi a^2$ [Newman (1977)], are substituted into Eqs. (19) and (18) to solve for the system trajectories. The added mass coefficients remain constant since the orientation of the cylinder will not change during their interaction. Three normalized vortex half-spans, $h(0)/\sqrt{ab} = 0.5, 0.75$, and 1.0, were considered with respect to three ellipse aspect ratios, $b/a = 2/3, 1$, and $3/2$. The resulting upper vortex trajectories are presented in the reference frame moving with the ellipse in Figs. 6(a)-(c) for the three cylinder shapes. Note that all the ellipses posses identical area, $\pi$, to exclude the effect of the body inertia. It is observed that when the aspect ratio of the cylinder increases from $2/3$

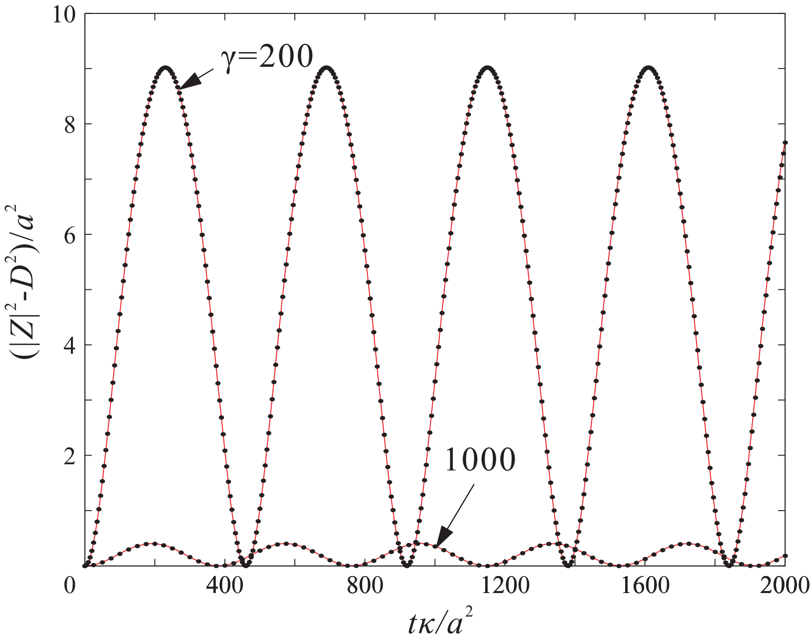


Figure 4: The square of the separation between the cylinder and vortex, $|Z|^2 = |\tilde{Z}^{(v)} - Z_c|^2$, as a function of normalized time. Thin lines and dots denote the results by the analytical equation, from (20), and the present numerical method.

to $3/2$, the vortex pair stretches more apparently when moving around the cylinder. At the vicinity of the cylinder, the impulse of the interior image vortex alone the negative $X_1$ increases that drives the cylinder to move to the right. When the vortex pair moves around the cylinder, the expansion of $h$ enhances its impulse and hence the cylinder is observed to decelerate and finally move towards the left in order to preserve the system total momentum. Finally, when vortex pair passed the cylinder, it dispatches some impulse onto the cylinder resulting in cylinder motion towards the positive direction. When the vortex pair moves sufficiently far downstream, the cylinder motion ceases and a finite lateral displacement to the right is found. The temporal trajectory of each cylinder with respect to various vortex configurations are shown in Figs. 7(a)-(b), using a dimensionless time, $\kappa t/(ab)$. The trajectory oscillation describes the aforementioned cylinder reverse motion when the vortex pair passed it. Comparing the nine cases, it can be concluded that greater cylinder displacement is developed when a fatter vortex (larger $h(0)$) interacts with a thinner ellipse. This may be attributed to a fatter pair possesses greater vortex impulse that enhances the cylinder motion and the added mass coefficient of a thinner ellipse is

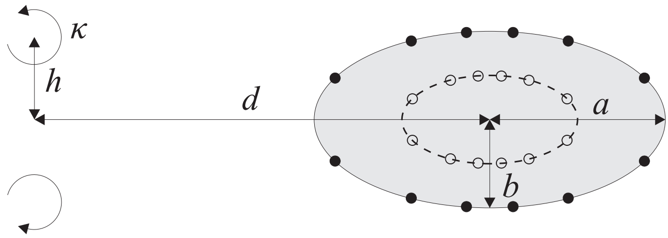


Figure 5: Schematic diagram of the axisymmetric approach of a vortex pair towards an elliptical cylinder. The initial distribution of the inner sources (open circles) and the collocation points (solid circles) is also depicted.

much lower that greatly diminishes the hindering force.

## 5 Conclusion

The force on an object of arbitrary shape in an inviscid, irrotational, and incompressible flow with the presence of flow singularities is calculated with the current method that integrates the MFS and the generalized Lagally theorem. In MFS, a singularity system is determined to achieve an user-specified error tolerance for the boundary condition via numerical iteration with the UNLSJ routine. The resulting singularity strength and configuration are employed to obtain the hydrodynamic force via algebraic calculations according to the generalized Lagally theorem. This force is then used to study the object-flow(singularity) interactions.

The current method is validated by the problem where a circular cylinder interacts with an external free vortex, the obtained data agree to the literature analytical results. The axisymmetric approach of a vortex pair towards an elliptical cylinder is then considered as a example involving with a non-circular object. The trajectory of the top vortex for three initial vortex configurations and three ellipse aspect ratios are given in the frame moving with the cylinder. The enhancement of the vortex stretching when moving around the cylinder with increasing aspect ratio is observed. The time evolution of the cylinder position further reveals greater cylinder displacement when a fatter vortex interacts with a thinner ellipse. Lastly, we would like to stress again that the true merit of the current scheme in computing the hydrodynamic force is it bypasses the surface integration that always introduces numerical error in conventional approaches. Although the present study considers exterior vortices only, it is straightforward to further include more external singularities of different types. Undoubtedly, it provides new means to study the fluid-structure interaction problems when the external flow can be feasibly approximated by an ideal flow.

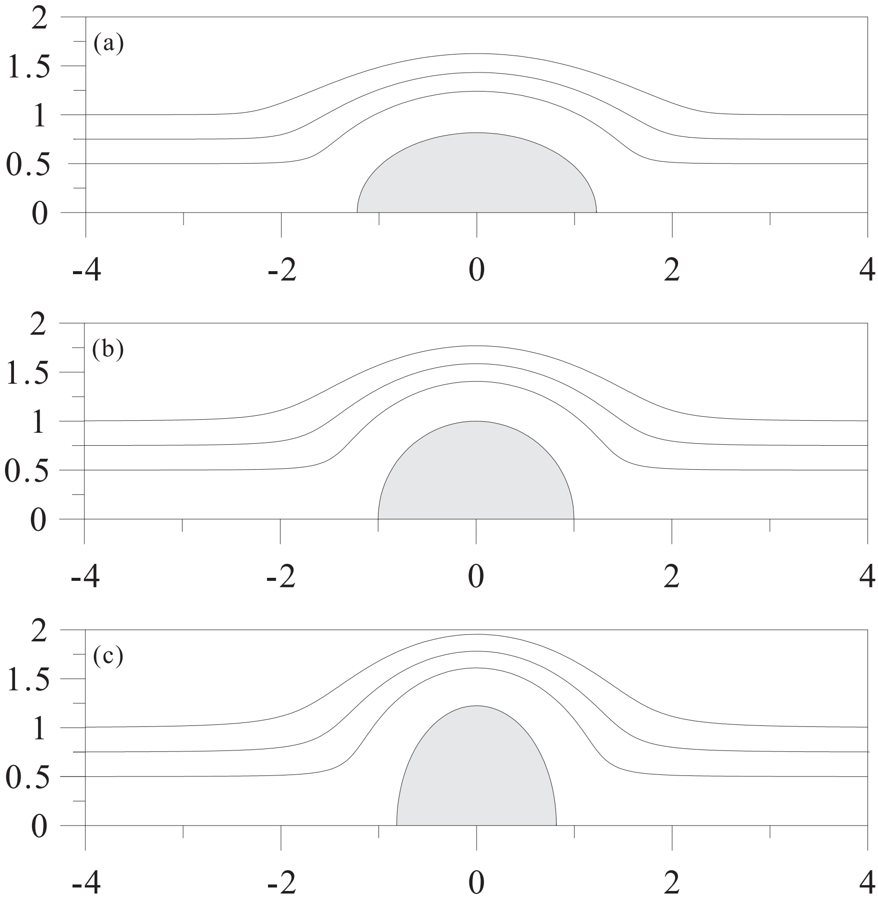


Figure 6: Trajectories of the top vortex for three ellipses with $b/a$ = (a)$2/3$, (b)1, and (c)$3/2$. For each case, three initial vortex half-spans, $h(0)/\sqrt{ab} = 0.5, 0.75, 1.0$, are considered.

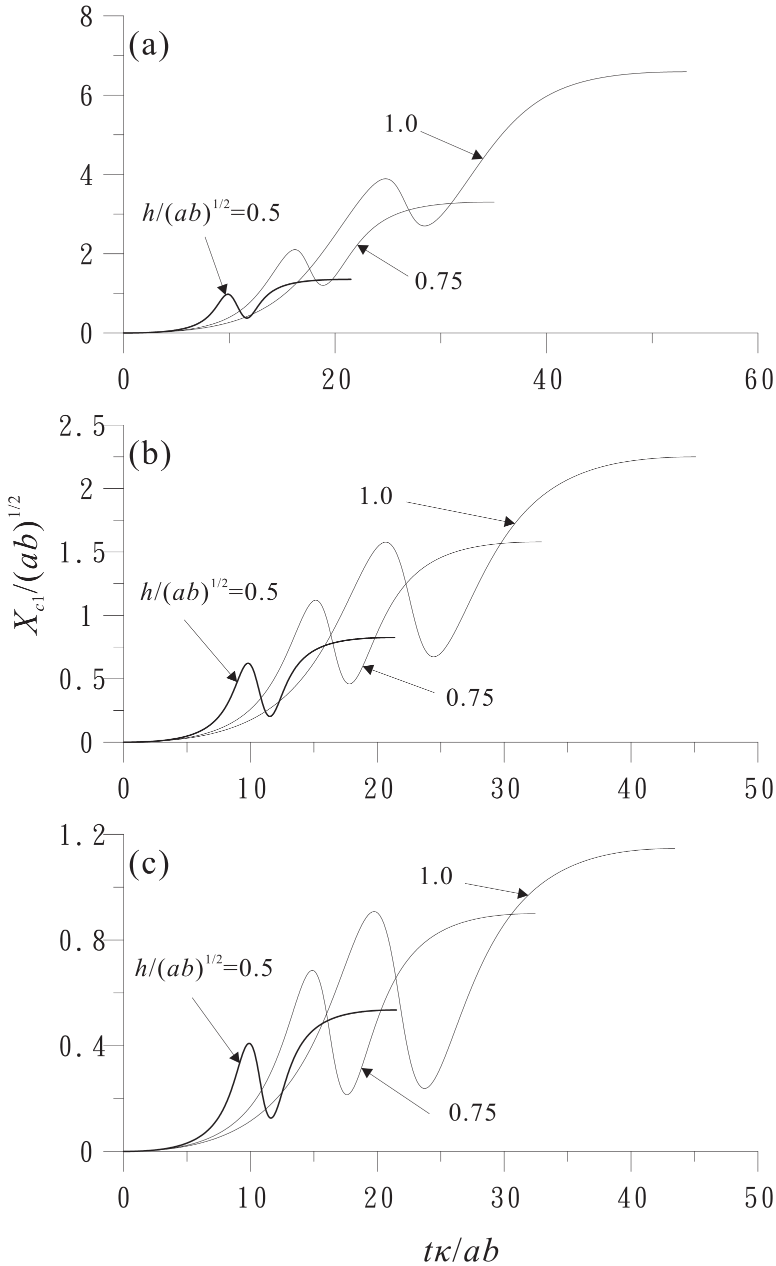


Figure 7: The position of the cylinder center, $X_c/\sqrt{ab}$, as a function of dimensionless time, $\kappa t/(ab)$ for different cylinder aspect ratios, $b/a =$ (a)$2/3$, (b)1, and (c)$3/2$. Three initial vortex half-spans, $h(0)/\sqrt{ab} = 0.5, 0.75, 1.0$, are considered for each case.

**Acknowledgement:** The authors would like to acknowledge the kind funding support from the National Science Council of Taiwan, through Grant NSC 97-2221-E-002-247-MY3, and the National Taiwan University, through Grant 99R80804.

## References

**Biesheuvel, A.** (1985): A note on the generalized Lagally theorem. *J. Eng. Math.*, vol. 19, pp. 69–77.

**Birkhoff, G.** (1950): *Hydrodynamics: a Study in Logic, Fact, and Similitude*. Princeton University Press.

**Cummins, W. E.** (1953): The forces and moments acting on a body moving in an arbitrary potential stream. *David Taylor Model Basin, rep. no. 708*.

**Eames, I.; Landeryou, M.; Flór, J. B.** (2007): Inviscid coupling between point symmetric bodies and singular distributions of vorticity. *J. Fluid Mech.*, vol. 589, pp. 33–56.

**Fairweather, G.; Karageorghis, A.** (1998): The method of fundamental solutions for elliptic boundary value problems. *Adv. Comput. Math.*, vol. 9, pp. 69–95.

**Fairweather, G.; Karageorghis, A.; Martin, P. A.** (2003): The method of fundamental solutions for scattering and radiation problems. *Eng. Anal. Bound. Elem.*, vol. 27, pp. 759–769.

**Golberg, M. A.; Chen, C. S.** (1998): The method of fundamental solutions for potential, Helmholtz and diffusion problems. In: M.A. Golberg, Editor, Boundary Integral Methods: Numerical and Mathematical Aspects, WIT Press/Computational Mechanics Publications, Boston, pp. 103–176.

**Gu, M. H.; Young, D. L.; Fan, C. M.** (2009): The method of fundamental solutions for one-dimensional wave equations. *CMC: Computers, Materials, & Continua*, vol. 11, pp. 185–208.

**Johnston, R. L.; Fairweather, G.** (1984): The method of fundamental solutions for problems in potential flow. *Appl. Math. Model.*, vol. 8, pp. 265–270.

**Kanso, E.; Oskouei, B. G.** (2008): Stability of a coupled body–vortex system. *J. Fluid Mech.*, vol. 600, pp. 77–94.

**Katsurada, M.** (1989): A mathematical study of the charge simulation method II. *J. Math. Sci.-Univ. Tokyo*, vol. 36, pp. 135–162.

**Lagally, M.** (1922): Berechnung der kräfte und momente die strömende flüssigkeiten auf ihre begrenzung ausüben. *Z. Angew. Math. Mech.*, vol. 2, pp. 409–422.

**Lamb, H.** (1932): *Hydrodynamics*. Dover Press.

**Landweber, L.** (1956): On a generalization of Taylor's virtual mass relation for rankine bodies. *Q. Appl. Math.*, vol. 14, pp. 51–56.

**Landweber, L.; Chwang, A. T.** (1989): Generalization of Taylor's added-mass formula for two bodies. *J. Ship Res.*, vol. 33, pp. 1–9.

**Landweber, L.; Miloh, T.** (1980): Unsteady Lagally theorem for muitipoles and deformable bodies. *J. Fluid Mech.*, vol. 96, pp. 33–46.

**Landweber, L.; Yih, C. S.** (1956): Forces, moments, and added masses for rankine bodies. *J. Fluid Mech.*, vol. 1, pp. 319–336.

**Lin, C. Y.; Gu, M. H.; Young, D. L.** (2010): The time-marching method of fundamental solutions for multi-dimensional telegraph equations. *CMC: Computers, Materials, & Continua*, vol. 18, pp. 43–68.

**Milne-Thompson, L. M.** (1968): *Theoretical Hydrodynamics*. Dover Press.

**Moré, J. J.; Garbow, B. S.; Hillstrom, K. E.** (1980): User guide for MINPACK-1. Argonne National Laboratory Report ANL-80-74, Argonne, III.

**Newman, J. N.** (1977): *Marine Hydrodynamics*. The MIT Press.

**Shashikanth, B. N.** (2006): Symmetric pairs of point vortices interacting with a neutrally buoyant two-dimensional circular cylinder. *Phys. Fluids*, vol. 18, pp. 127103.

**Taylor, G. I.** (1928): The energy of a body moving in an infinite fluid, with an application to airships. *Proc. Roy. Soc. London Ser. A*, vol. 120, pp. 13–21.

**Wang, J. G.; Ahmed, M. T.; Leavers, J. D.** (1990): Nonlinear least squares optimization applied to the method of fundamental solutions for eddy current problems. *IEEE Trans. Magn.*, vol. 26, pp. 2385–2387.

**Wu, C. T.; Yang, F.-L.; Young, D. L.** (2011): Generalized two-dimensional Lagally theorem with free vortices and its application to fluid-body interaction problems. *J. Fluid Mech.* (Revised).

**Yang, F.-L.; Wu, C. T.; Young, D. L.** (2011): On the calculation of two-dimensional added mass coefficients by the Taylor theorem and the method of fundamental solutions. *J. Mech.* (Accepted).

**Yih, C. S.** (1977): *Fluid mechanics* : *a concise introduction to the theory*. West River Press.

**Young, D. L.; Tsai, C. C.; Lin, Y. C.; Chen, C. S.** (2006): The method of fundamental solutions for eigenfrequencies of plate vibrations. *CMC: Computers, Materials, & Continua*, vol. 4, pp. 1–10.